IEEE Access
Multidisciplinary | Rapid Review | Open Access Journal

Received October 16, 2021, accepted November 5, 2021, date of publication November 8, 2021,
date of current version November 24, 2021.

Digital Object Identifier 10.1109/ACCESS.2021.3126764

A Refined Load Distribution Method for Large Hydropower Stations With Multiple Units Considering Constraints of Substations

XIAO CHEN, JIANZHONG ZHOU, AND BENJUN JIA
School of Civil and Hydraulic Engineering, Huazhong University of Science and Technology, Wuhan 430074, China
Hubei Key Laboratory of Digital Valley Science and Technology, Wuhan 430074, China

Corresponding author: Jianzhong Zhou (jz.zhou@hust.edu.cn)

This work was supported by the Key Project of the Natural Science Foundation of China under Grant U1865202 and Grant 52039004.

ABSTRACT Large hydropower stations often undertake peak regulation tasks during the non-abandoning water season. This requires a reasonable arrangement of unit commitment and load distribution (UCLD). In this study, a load distribution model considering constraints of substations was established, and a novel refined and practical method (RPM) was proposed by considering a whole plant-substation module, substation-unit module, and adjustment module along with practical strategies. The Three Gorges hydropower station in China was selected to demonstrate the effects of the RPM. The results showed that the RPM with high calculation timeliness can obtain UCLD schemes with high rationality and practicability under the constraints of the whole plant, substations, and units. The relative mean absolute error of the simulation outflow could be controlled within 1%, thereby providing a valuable reference for forecasting the outflow process which involving the unit level.

INDEX TERMS Large hydropower stations, load distribution, substation constraints, output adjustment strategies, bus connection switching status.

I. INTRODUCTION

In the context of carbon emissions peaks [1] and carbon neutrality [2], the energy structures and industrial layouts of various countries have changed to different degrees. In recent years, the installed capacities of new energy sources such as wind and solar energy have been growing rapidly in China [3]. However, the uncontrollability and randomness caused by their grid-connected operations also pose a significant threat to the security and stability of the grid [4]. Hydroelectric energy is a type of clean and conventional energy with a flexible peak regulation capacity, and is generally a superior choice for addressing with these difficult problems [5]. Therefore, studying the operation management of hydropower stations is of great significance for optimizing the national energy structure, smoothly promoting the connection of new energy sources with the grid, and gradually realizing the goal of carbon neutrality.

The associate editor coordinating the review of this manuscript and approving it for publication was Xujie Li.

Large hydropower stations often undertake peak regulation tasks from the grid, and are expected to carry out the load instructions strictly, arrange unit commitment and load distribution (UCLD) reasonably, and adapt to load fluctuations quickly [6], [7]. UCLD is a typical nonlinear large-scale optimization problem with complex constraints [8], [9]. The computation burden of UCLD grows exponentially with an increase in hydro units. Cheng *et al.* [10] pointed out that when the number of hydro units is greater than 10, a dimensionality disaster occurs. In the past few decades, a large number of studies have attempted to solve the UCLD problem; these studies can be broadly divided into three categories.

The first category is the traditional methods, mainly including lagrangian relaxation (LR) [11], [12], nonlinear programming (NLP) [13], mixed integer linear programming (MILP) [14], [15] and dynamic programming (DP) [10], [16]. These methods have gained elegant achievements for specific scenarios with simple constraints and small scales. However, their respective flaws are the main obstacles for the extensive application. LR can achieve a quick solution, but it is generally difficult to find suitable lagrange multipliers [17].

Nonlinearity is a prominent feature of the UCLD problem, and is mainly caused by the dynamic operation characteristics of hydro units. Taktak and D'Ambrosio [18] summarized that NLP is a very efficient method to model and solve the UCLD model. However, it is not easy to manage the nonlinearity of NLP in general, as approaches tend to be mainly limited by the scale of the problem and solving tools. While MILP can be aided by normalized and efficient commercial software solvers, such as LINGO and CPLEX. More importantly, there is no limit to the size of the problem. Li *et al.* [19] utilized MILP to optimize the hydro unit commitment. However, linearization has an extreme influence on the solution feasibility. Especially for large hydropower stations with numerous units and complex constraints, the poor quality of linearization can easily lead to unsatisfactory dispatching results [18]. Along with MILP, DP has been one of the most classical algorithms for solving the UCLD model. More importantly, it is skilled in addressing nonlinear optimization problems. But with an increase in units, the calculation efficiency of DP decreases sharply [10].

The second category includes heuristic methods, such as the particle swarm optimization [10], [20], ant colony algorithm [21]–[23], genetic algorithm [24], [25], evolutionary programming [26], [27], and differential evolution [28], [29]. These algorithms usually determine a suboptimal solution by simulating a specific natural phenomenon. In general, the modeling steps can be divided into three steps. First, the sequence of the unit on-off states during the dispatching period is abstracted into a single particle, and an initial population is generated. Second, the iteration and update rules of the population are defined according to different natural phenomena, and constraint-handling strategies are formulated. Finally, the rules and strategies are executed until the termination conditions are met. Compared with traditional methods, heuristic methods have powerful searching abilities and high calculation timeliness [30]. However, the dispatching results are often not convergent, leading to deep confusion regarding the actual dispatching decisions of hydropower stations; this has become the main obstacle to their application in production practice [31].

The third category includes methods with practical strategies. Based on a detailed analysis of the operation characteristics of the target hydropower station, the concerns affecting the dispatching results are analyzed, and practical methods are proposed. For example, Cristian Finardi *et al.* [32] proposed a two-phase decomposition strategy to yield accurate and practical results for the UCLD in the Brazilian regulatory framework. Siu *et al.* [33] designed the hierarchical approach to determine the optimal hydroelectric unit generation schedules. Li and Tang *et al.* [34] used Xiluodu as the research object, and proposed a practical method for increasing and decreasing the type and number of hydro units under varying load conditions. Zhou *et al.* [35] proposed a load-adjustment method with regime-changing conditions for the Yuanshui cascade hydropower stations in China. Methods with practical strategies such as these can be regarded as summaries of practical dispatching problems; in general, they greatly improve the solution efficiency for the UCLD problem, and have strong engineering application value. In contrast to the first two categories, proposals of this type of method require a full analysis and understanding of the case, and the effects and performances also need to be repeatedly verified [36].

In recent years, a large number of large hydropower stations have been successively put into operation in China, such as Wudongde and Baihetan [37], [38]. Large hydropower stations with multiple hydro units are often divided into several substations according to the relative positions of the units. Moreover, different substations are usually connected to different outgoing transmission lines, and the constraints for the substations from the grid and those from the substations themselves are not identical. Previous studies on the UCLD problem have considered many constraints; these all can be divided into a constraint set for the hydropower station level (CS-HSL) and a constraint set for the unit level (CS-UL). However, so far there hasn't been a method to deal with the UCLD problem considering the constraint set of the substation level (CS-SL) (hereafter the ''UCLD-SC''). Hence, this has led to new and urgent requirements for power generation enterprises to strengthen the refined dispatching and management levels of hydropower stations, and to consider the substations constraints when modeling the UCLD problem; this is the main motivation of this study. In this study, the UCLD-SC model is established and a novel refined and practical method (RPM) is proposed for the first time. The Three Gorges hydropower station (TGHS) is selected as a case study for verifying the high applicability and timeliness of the RPM.

The remainder of this paper is organized as follows. Section II introduces the study case. Section III describes the UCLD-SC model, including the objective function, constraint sets, and other modeling principles. Section IV introduces the RPM in detail. Section V presents the test results and discussion, and Section VI summarizes the conclusions of this study.

II. STUDY AREA AND HYDRO UNIT LAYOUT

The Three Georges Water Conservancy Project (TGWCP) is located on the main stream of the Yangtze River in China [39]. Gezhouba [40], with daily regulation capacity, is located 38 km downstream from the dam site of the TGWCP, and has a remarkable jacking effect for the TGHS. The locations of the TGWCP and Gezhouba are shown in Figure 1, and the engineering layout of the hydro units in the TGHS is presented in Figure 2. As shown in Figure 2, the TGHS is equipped with 34 units; these belong to nine different types (marked with different colors). According to the layout of the units and connection mode of the outgoing transmission lines, the units are divided into four substations: the power substation, left bank substation, right bank substation, and land substation. Moreover, these four substations are physically independent from each other. In particular, there are two bus connection switches distributed in the left and right

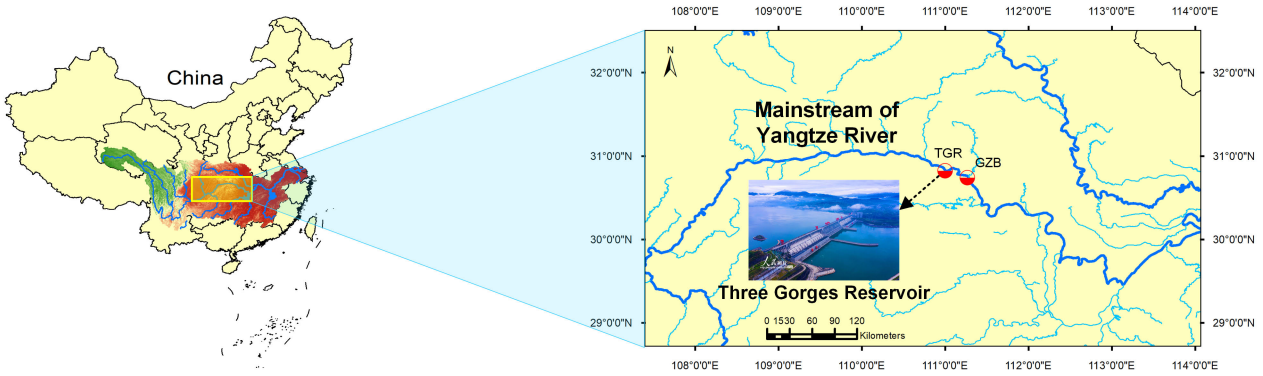

FIGURE 1. Locations of the three Georges water conservancy project (TGWCP) and Gezhouba.

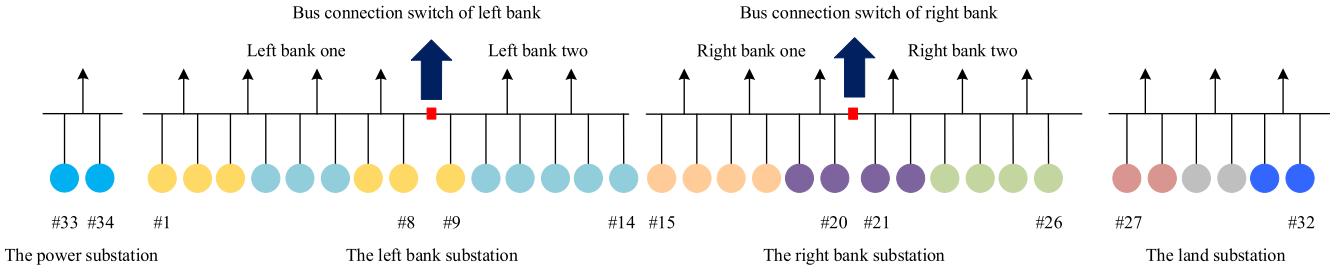

FIGURE 2. Engineering layout of hydro units in the TGWCP.

substations, and the on-off state of each switch is restricted by the grid. The main reason for choosing the TGHS as the study case is that it has the largest number of substations and the most complex constraints. Meanwhile, it also has the unique problem of the bus connection switch. The other large hydropower stations mentioned in the introduction section are simplified cases of the TGHS.

III. PROBLEM FORMULATION

Based on the investigations from Three Gorges Cascade Dispatch & Communication Center (TGCDCC) [41], which governs the TGHS, the optimal operation efficiency of the hydro units is often not pursued deliberately in the actual dispatching, that is, the hydropower stations do not always maintain the minimum water consumption conditions for a given load. There are two main reasons for this phenomenon. First, the operations of the hydro units are restricted by the grid, and cannot maintain the optimal operation conditions at all times. Second, from the perspective of safety, for both the grid and hydropower station, it is desired that the outputs of units are relatively stable. Hence, the goal of the UCLD-SC is to determine a suboptimal dispatching scheme in which UCLD are reasonably arranged. The objective function [10] is defined as follows. (The modeling variables in this paper can be viewed in Appendix.)

A. OBJECTIVE FUNCTION

$$\tilde{\min}\ Q(N) = \sum_{t=1}^{T} \sum_{i}^{I} u_{i,t} Q_{i,t}(H_{i,t}, N_{i,t}) + Q_t^{sup} \quad (1)$$

$$N = [N_1, N_2, N_t, \cdots, N_T] \quad (2)$$

Notably, the time scope of this study does not include the abandoning water season.

B. CONSTRAINTS

After discussions with the site dispatchers in the TGCDCC, all of the concerned constraints are considered and grouped into the triple constraint sets. Different constraints have different degrees of importance. The important constraints are treated as rigid constraints, i.e., the dispatching results should obey them. The soft constraints are marked directly when introduced. Soft constraints are of less importance to the solution, and may have a significant influence on the feasibility of the solution. When a feasible solution cannot be found, the soft constraints should not be considered.

1) CONSTRAINT SET-HYDROPOWER STATION LEVEL (CS-HSL)

(1) Water balance constraint

$$V_t = V_{t-1} + (I_t - Q_t) \cdot \Delta t \quad (3)$$

(2) Load-balance constraint

$$N_t = \sum_{k=1}^{K} N_{k,t} = \sum_{k=1}^{K} \sum_{j=1}^{J} N_{k,j,t} = \sum_{i=1}^{I} N_{i,t} \quad (4)$$

$$J = J(k) \quad (5)$$

Here, we number the same units from the perspectives of the whole plant and substation to make the subsequent statements clearer.

(3) Forebay water level (FWL) constraint

$$Z_L \le Z_t \le Z_U \tag{6}$$

(4) Outflow constraint

$$Q_L \le Q_t \le Q_U \tag{7}$$

(5) Output constraint

$$N_L \le N_t \le N_U \tag{8}$$

(6) Amplitude of the water level fluctuation constraint

$$Z_t - Z_{t-1} \le Z_{rise}^{bear} \tag{9}$$

$$Z_t - Z_{t-1} \le -Z_{drop}^{bear} \tag{10}$$

(7) Output constraint restricted by the grid

$$N_t \le N_{max}^{grid} \tag{11}$$

(8) Maximum operational number constraint of units

$$\sum_{i=1}^{I} u_{i,t} \le Num_{max}, \quad t = 1, 2, \cdots, T \tag{12}$$

This constraint is the first soft constraint. The operation efficiency is relatively high when units operate around the rated output. Therefore, the operating number of units should be limited.

2) CONSTRAINT SET-SUBSTATION LEVEL (CS-SL)

(1) Bus connection switch constraint

$$S_L, S_R = \{S_{on}, S_{off}\} \tag{13}$$

(2) Minimum operational unit number constraint of substations

$$\sum_{j=1}^{J} u_{k,j,t} \ge Num_k^{min}, \quad k = 1, 2, \cdots, K \tag{14}$$

This constraint is another soft constraint. It can avoid obtaining a solution in which the output of the entire plant is excessively concentrated in certain substations while the output of the other substations is almost zero.

(3) Stable operation zone (SOZ) constraint of substations

The operation area of a hydro unit can be divided into a SOZ and forbidden operation zone (FOZ). The SOZs of units in TGHS are all continuous. For example, Figure 3 shows the distribution of the SOZ and FOZ for Unit 3 in the left bank substation. If a gross water head is not exactly equal to the ordinate values in Figure 3, gross water head and bounds of SOZ will be calculated by linear interpolation.

In view of this, the SOZs of substations can be expressed as follows:

$$\sum_{j=1}^{J} u_{k,j,t} L_{k,j}(H_t^{gross}) \le N_{k,t} \le \sum_{j=1}^{J} u_{k,j,t} U_{k,j}(H_t^{gross}) \tag{15}$$

$$H_t^{gross} = (Z_t + Z_{t-1})/2 - Z_t^{tail} \tag{16}$$

Notably, the empirical formula for Q_t and the water difference is often utilized to determine Z_t^{tail} in the TGCDCC at present; the definition is shown in Equation (17).

$$\Delta Z_t = Z_t^{tail} - Z_t^{gzb} = \Delta Z(Q_t) \tag{17}$$

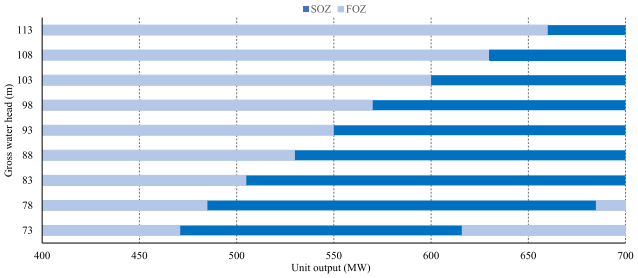

FIGURE 3. Distribution of stable operation zone (SOZ) and forbidden operation zone (FOZ) for unit 3 in the left bank substation.

3) CONSTRAINT SET-UNIT LEVEL (CS-UL)

Except for nonlinearity, the combinatorial aspect and discontinuous characteristics are the other two major characteristics of the CS-UL. The combinatorial aspect is caused by discrete factors such as the on-off states of the units, and the discontinuity is limited by the FOZs of the units [42]–[44].

(1) Repair planning constraints

$$Re_i = \{Re_{on}, Re_{off}\}, \quad i = 1, 2, \cdots, I \tag{18}$$

If unit i is in the repair state, $u_{k,j,t}$ and $u_{i,t}$ are both set to 0.

(2) Minimum uptime/downtime constraint

$$\begin{cases} T_{i,t}^{on} \ge T_i^{up} \\ T_{i,t}^{off} \ge T_i^{down} \end{cases} \tag{19}$$

This is the third soft constraint, and is used to avoid frequent unit starts and stops to a certain extent.

(3) Gross water head constraint

$$H_L \le H_t^{gross} \le H_U \tag{20}$$

(4) SOZ constraint of units

$$L_{k,j}(H_t^{gross}) \le N_{k,j,t} \le U_{k,j}(H_t^{gross}) \tag{21}$$

(5) Maximum output constraint of units

$$N_{k,j}^{max}(H_t^{gross}) = \min\left\{N_{k,j}^{rated}, N_{k,j}^{exp}(H_t^{gross}), U_{k,j}(H_t^{gross})\right\} \tag{22}$$

C. OTHER MODELING PRINCIPLES IN UCLD-SC

According to the site investigation, except for the triple constraint sets in Section III-B, the modeling of the UCLD-SC also needs to meet certain load distribution and unit operation principles, as follows. Principle-I: The units of the TGHS should operate to exceed 70% of the expected output (i.e., 490 MW), as guided by the manufacturer's instructions. Principle-II: the units should not frequently cross between the SOZ and FOZ. Principle-III: Load fluctuations with a small amplitude should be handled by the units currently in operation as much as possible.

IV. METHODOLOGY

When the UCLD-SC contains triple constraint sets, there are three levels of output from the hydropower stations, i.e., the outputs of the entire plant, substations, and units. Therefore, we divide the solving method into two modules: the whole plant-substation module (WPSM) and substation-unit module (SUM), in which the WPSM determines the initial output of each substation, and SUM determines UCLD. Notably, the initial output of substations as determined by the WPSM may not satisfy the SOZ constraint of substations, which is a focus in the RPM. Therefore, an adjustment module with practical strategies (AM-PS) is proposed for adjusting the output of substations. The details of these modules and the overall flowchart are described in the following sections.

A. WHOLE PLANT-SUBSTATION MODULE (WPSM)

The central distribution principles of WPSM are that the condition of UCLD should keep as stable as possible between periods, namely the Principle-III in Section III-C. When the load fluctuation is large, it should be jointly undertaken by substations. In this way, output of all the substations can vary relatively smoothly, which is beneficial to safe operation. The specific steps of the WPSM at period t are as follows.

(1) Firstly, gain $N_{k,t}^{ini}$ by statistics, and assign it to $N_{k,t}^{temp}$, namely Equation (23). Then, count ΔN_t by Equation (24). $N_{k,t}^{ini}$ is the initial output, therefore, it can be regarded as a determinate quantity at the beginning of period t. As for $N_{k,t}^{temp}$, it is used to record output results of substations distributed by WPSM. The purpose of WPSM is to distribute ΔN_t between substations until it is equal to 0.

$$N_{k,t}^{temp} = N_{k,t}^{ini} \tag{23}$$

$$\Delta N_t = N_t - \sum\nolimits_{k=1}^{K} N_{k,t}^{ini} \tag{24}$$

(2) Calculate $N_k^{max}(H_t^{gross})$ and $N_k^{diff}(H_t^{gross})$.

$$N_k^{max}(H_t^{gross}) = \sum\nolimits_{j=1}^{J} N_{k,j}^{max}(H_t^{gross}), \quad Re_{k,j} = Re_{on} \tag{25}$$

$$N_k^{diff}(H_t^{gross}) = N_k^{max}(H_t^{gross}) - N_{k,t}^{temp} \tag{26}$$

The $N_k^{diff}(H_t^{gross})$ is the difference from $N_{k,t}^{temp}$ to $N_k^{max}(H_t^{gross})$, and can show the loading condition of substations.

(3) Calculate $N_{k,pre}^{max}(H_t^{gross})$ and $N_{k,pre}^{min}(H_t^{gross})$.

$$N_{k,pre}^{max}(H_t^{gross}) = \sum\nolimits_{j=1}^{J} s_{k,j,t-1} N_{k,j}^{max}(H_t^{gross}), \quad k = 1, 2, \cdots, K \tag{27}$$

$$N_{k,pre}^{min}(H_t^{gross}) = \sum\nolimits_{j=1}^{J} s_{k,j,t-1} L_{k,j}(H_t^{gross}), \quad k = 1, 2, \cdots, K \tag{28}$$

$$\boldsymbol{s}_{k,t-1} = [s_{k,1,t-1}, s_{k,2,t-1}, \cdots, s_{k,J,t-1}] \tag{29}$$

Here, the parameter of unit commitment is $\boldsymbol{s}_{k,t-1}$. If the unit commitment at period t-1 satisfy output requirements at period t, the unit commitment will remain original. This obeys the Principle-III in Section III-C.

(4) Check the SOZ constraint of substations under H_t^{gross} and $\boldsymbol{s}_{k,t-1}$ by Formula (30). For substations in *FSS*, calculate $N_k^{dec}(H_t^{gross})$ and $N_k^{inc}(H_t^{gross})$, which can be regarded as adjustable output spaces, and show the ability of decreasing and increasing output at substation k, respectively.

$$N_{k,pre}^{min}(H_t^{gross}) \le N_{k,t}^{temp} \le N_{k,pre}^{max}(H_t^{gross}), \quad k = 1, 2, \cdots, K \tag{30}$$

$$N_k^{dec}(H_t^{gross}) = N_{k,t}^{temp} - N_{k,pre}^{min}(H_t^{gross}), \quad k \in FSS \tag{31}$$

$$N_k^{inc}(H_t^{gross}) = N_{k,pre}^{max}(H_t^{gross}) - N_{k,t}^{temp}, \quad k \in FSS \tag{32}$$

(5) Discretize ΔN_t by N_{step}, and allocate N_{step} according to $N_k^{dec}(H_t^{gross})$ and $N_k^{inc}(H_t^{gross})$. Specifically, if ΔN_t is positive, find the substation with $R^{inc}(H_t^{gross})$, and add N_{step} to it; if ΔN_t is negative, find the substation with $R^{dec}(H_t^{gross})$, and subtract N_{step} from it, namely Equation (35). This distribution step is called as the one-step output adjustment.

$$R^{dec}(H_t^{gross}) = \max\{N_k^{dec}(H_t^{gross})/N_{k,pre}^{max}(H_t^{gross})\}, \quad k \in FSS \tag{33}$$

$$R^{inc}(H_t^{gross}) = \max\{N_k^{inc}(H_t^{gross})/N_{k,pre}^{max}(H_t^{gross})\}, \quad k \in FSS \tag{34}$$

$$\begin{cases} N_{k,t}^{temp} = N_{k,t}^{temp} + N_{step}, k \ with \ R^{inc}(H_t^{gross}), & if \ \Delta N_t > 0 \\ N_{k,t}^{temp} = N_{k,t}^{temp} - N_{step}, k \ with \ R^{dec}(H_t^{gross}), & if \ \Delta N_t < 0 \end{cases} \tag{35}$$

After conducting the one-step output adjustment for one time, update ΔN_t by Equation (36). Then, update $N_k^{diff}(H_t^{gross})$ by Equation (26), $N_k^{dec}(H_t^{gross})$ and $N_k^{inc}(H_t^{gross})$ by Equation (31) and Equation (32). Whereafter, update $R^{dec}(H_t^{gross})$ and $R^{inc}(H_t^{gross})$ by Equation (33) and Equation (34).

$$\Delta N_t = \begin{cases} \Delta N_t - N_{step}, & \Delta N_t > 0 \\ \Delta N_t + N_{step}, & \Delta N_t < 0 \end{cases} \tag{36}$$

The process of the one-step output adjustment is terminated until ΔN_t is equal to zero or the adjustable output spaces have been run out. Then, ΔN_t^{sum} can be calculated by Equation (37).

$$\Delta N_t^{sum} = \sum\nolimits_{m=1}^{M} N_{step} \tag{37}$$

The adjustable output spaces can maintain the original unit commitment state, deal with ΔN_t, and avoid frequent switching of units, namely the Principle-II in Section III-C.

(6) Check the value of ΔN_t. If ΔN_t is equal to zero, the WPSM process is terminated. Otherwise, the remaining ΔN_t is allocated by the one-step output adjustment with Equation (38) until it is equal to 0. Specifically, if ΔN_t is positive, find the substation with the $R_{max}^{diff}(H_t^{gross})$ (i.e., Equation (39)) and add N_{step} to it (The $R_{max}^{diff}(H_t^{gross})$ means the substation undertakes the lightest output, and owns the priority to increase output.); if ΔN_t is negative, find the substation with the $R_{min}^{diff}(H_t^{gross})$, and subtract N_{step} from it. (The $R_{min}^{diff}(H_t^{gross})$ means the substation undertakes the heaviest output, and

owns the priority to decrease output.). In addition, the design of the Step (6) can let the minimum operational unit number constraint of substations (i.e., Formula (14)) hold in general.

The allocation of the remaining ΔN_t obey the central distribution principles of WPSM, but it doesn't consider the SOZ range of substations. Hence, it's possible that $N_{k,t}^{temp}$ violate the SOZ constraint.

$$\begin{cases} N_{k,t}^{temp} = N_{k,t}^{temp} + N_{step}, k \text{ with } R_{max}^{diff}(H_t^{gross}), & if\ \Delta N_t > 0 \\ N_{k,t}^{temp} = N_{k,t}^{temp} - N_{step}, k \text{ with } R_{min}^{diff}(H_t^{gross}), & if\ \Delta N_t < 0 \end{cases} \tag{38}$$

$$R_{max}^{diff}(H_t^{gross}) = \max\{N_k^{diff}(H_t^{gross})/N_k^{max}(H_t^{gross})\}, \quad k = 1, \cdots, K \tag{39}$$

$$R_{min}^{diff}(H_t^{gross}) = \min\{N_k^{diff}(H_t^{gross})/N_k^{max}(H_t^{gross})\}, \quad k = 1, \cdots, K \tag{40}$$

Thus far, the WPSM processes have been introduced. The installed capacities of substations are different, so the one-step output adjustment in Step (5) and (6) both use relative indicators to allocate load fluctuations. The flowchart of WPSM is as follows:

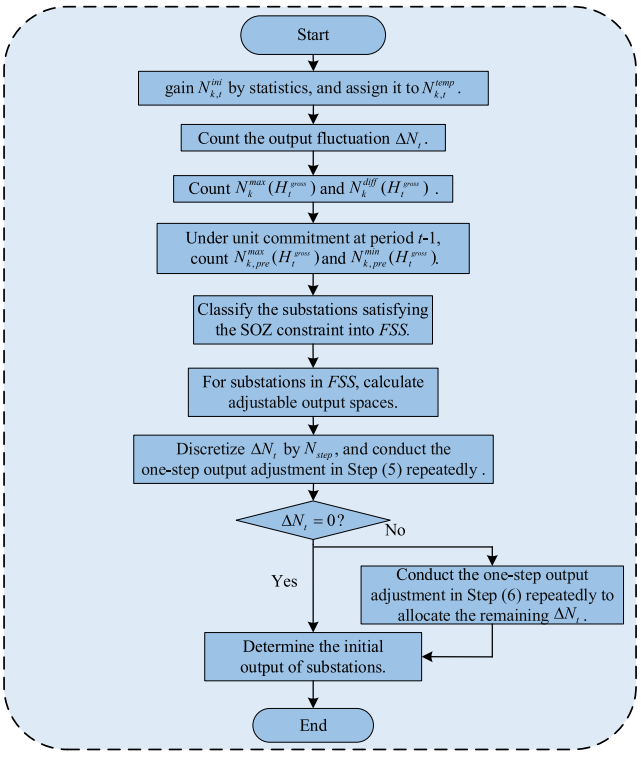

FIGURE 4. Flowchart of whole plant-substation module (WPSM).

B. SUBSTATION-UNIT MODULE (SUM)

There are three categories of methods can be used to determine the UCLD. Here, the UCLD should be determined with stability and high timeliness. Simultaneously, all units need to operate in high efficiency zones. Heuristic methods are excluded because results not convergent. While, the third category methods with practical strategies are proposed with difficulty to determine UCLD for so many constraints. They are more skilled in designing solution framework, namely the RPM in this paper. In the traditional methods, except the high timeliness, DP perfectly satisfies the solution requirements of UCLD-SC with 34 units. Jia *et al.* [45] worked out the optimal load allocation table (OLAT) for the whole plant (OLAT-WP) with the aim of minimizing the streamflow consumption by using DP (Here, the Principle-I in Section III-C can be satisfied easily.), and quickly calculated the output and outflow by consulting the OLAT-WP. More fortunately, Lu *et al.* [36] has already proved a generalization theorem regarding the optimization principle, and showed that a lookup based on the OLAT-WP could also achieve the optimal allocation under any unit commitment. Here, the specific meaning of any unit commitment reflects the maintenance of units, and some units cannot participate in the load distribution. This discovery leads to an important conclusion that solving the UCLD-SC requires only one OLAT that contains all of the units, namely, the OLAT-WP. When the output and unit commitment of a substation are known, the load distribution of units can be determined by looking up the OLAT-WP under the assumption that the units of other substations are in the repairing state. Simultaneously, considering the shortcomings of other traditional methods mentioned in the introduction, DP and looking up the OLAT-WP become the optimal choice.

Without loss of generality, it is assumed that units l and m are the units of other substations, and are set in the repair state. If $N_{k,t}$ is equal to P_0, the following steps illustrate how to allocate it to the units in substation k, excluding units l and m.

(1) Select row P at the OLAT-WP.

(2) Excluding unit l and unit m, calculate the total output at row P, and mark it as P_1.

$$P_1 = \sum_{j=1}^{J} N_{k,j}^{P}, \quad j \neq l, m \tag{41}$$

(3) If $P_1 = P_0$, the output of units in row P is desired.

$$N_{k,j,t} = N_{k,j}^{P}, \quad j \neq l, m \tag{42}$$

If $P_1 < P_0$, P_1 is less than $N_{k,t}$. Turning to the next row, $P = P + 1$. Let $P_2 = P_1$, and return to Step (2); if $P_1 > P_0$, P_1 is larger than $N_{k,t}$, and utilize the following linear interpolation formula to obtain $N_{k,j,t}$. Hence, the load distribution of substation k is determined.

$$N_{k,j,t} = N_{k,j}^{P} - \frac{N_{k,j}^{P} - N_{k,j}^{P-1}}{p_1 - p_2}, \quad j \neq l, m \tag{43}$$

C. ADJUSTMENT MODULE WITH PRACTICAL STRATEGIES (AM-PS)

After the adjustment of AM-PS, the outputs of substations will meet the SOZ constraint, and the unit commitment is also determined, so that the SUM can be directly invoked to determine output of units. The steps of AM-PS are as follows.

(1) According to the value of $N_{k,t}^{temp}$ as determined by WPSM, the switching operation is executed for the units,

and the unit commitment $s_{k,t}$ at period t is determined. If $N_{k,t}^{temp} < N_{k,pre}^{min}(H_t^{gross})$, some units need to be turned off, whereas if $N_{k,t}^{temp} > N_{k,pre}^{max}(H_t^{gross})$, some units need to be turned on. In this study, the switching priority of the units is determined by the efficiency of the units at the expected output [17]. Specifically, the unit with the highest efficiency has the highest priority for startup, and the unit with the lowest efficiency has the highest priority for shutdown. Owing to the discontinuity of the SOZ, the startup operation can only ensure that the upper bound of the SOZ of the substation is higher than $N_{k,t}^{temp}$, whereas the shutdown operation can only ensure that the lower bound of the SOZ of the substation is less than $N_{k,t}^{temp}$. When conducting the switching operation, the relative position relation between $N_{k,t}^{temp}$ and the bounds of the SOZ is shown in Figure 5.

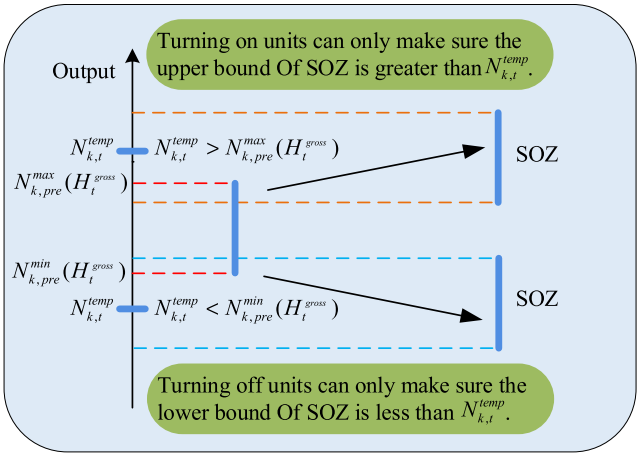

FIGURE 5. Relative position relation between $N_{k,t}^{temp}$ and bounds of SOZ when conducting switching operation of units.

(2) Under the unit commitment $s_{k,t}$, the feasible output range at period t is calculated.

$$N_{k,S}^{max}(H_t^{gross}, s_{k,t}) = \sum_{j=1}^{J} s_{k,j,t} N_{k,j}^{max}(H_t^{gross}) \quad (44)$$

$$N_{k,S}^{min}(H_t^{gross}, s_{k,t}) = \sum_{j=1}^{J} s_{k,j,t} L_{k,j}(H_t^{gross}) \quad (45)$$

(3) Utilize Formula (46) to verify that $N_{k,t}^{temp}$ satisfies the SOZ constraint of substation k. Directly invoke the SUM to determine output of units if the condition holds, and terminates the calculation of period t. Otherwise, the process proceeds to Step (4).

$$N_{k,S}^{min}(H_t^{gross}, s_{k,t}) \le N_{k,t}^{temp} \le N_{k,S}^{max}(H_t^{gross}, s_{k,t}), \quad k = 1, 2, \cdots, K \quad (46)$$

(4) For substations in Sub_t^{out}, calculate $Diff_{k,t}$ by Equation (47). For substations in Sub_t^{in}, calculate the adjustable output spaces by Equation (48) and Equation (49).

$$Diff_{k,t} = \begin{cases} N_{k,S}^{min}(H_t^{gross}) - N_{k,t}^{temp}, \\ \quad if\ N_{k,t}^{temp} < N_{k,S}^{min}(H_t^{gross}) \\ N_{k,t}^{temp} - N_{k,S}^{max}(H_t^{gross}), \\ \quad if\ N_{k,t}^{temp} > N_{k,S}^{max}(H_t^{gross}), \end{cases} \quad k \in Sub_t^{out} \quad (47)$$

$$N_{k,S}^{dec}(s_{k,t}) = N_{k,t}^{temp} - N_{k,S}^{min}(H_t^{gross}), \quad k \in Sub_t^{in} \quad (48)$$

$$N_{k,S}^{inc}(s_{k,t}) = N_{k,S}^{max}(H_t^{gross}) - N_{k,t}^{temp}, \quad k \in Sub_t^{in} \quad (49)$$

(5) Iterates through Sub_t^{out}, and adjust output of substations in Sub_t^{out} to satisfy the SOZ constraint. Similarly, discretize $Diff_{k,t}$ by N_{step}, and execute the one-step output adjustment repeatedly until $Diff_{k,t}$ is equal to zero or the adjustable output spaces have been run out. The $Diff_{k,t}$ is updated by Equation (50).

$$Diff_{k,t} = \begin{cases} Diff_{k,t} + N_{step}, & if\ Diff_{k,t} < 0 \\ Diff_{k,t} - N_{step}, & if\ Diff_{k,t} > 0 \end{cases} \quad (50)$$

When substation k executes the shutdown operation and not satisfy the SOZ constrain, $N_{k,t}^{temp}$ is bound to be larger than the upper bound of SOZ, and needs to be adjusted to this bound, whereas the remaining substations in Sub_t^{in} need to increase the output. Then, find the substation with $R_S^{inc}(s_{k,t})$, and add N_{step} to it, namely Equation (53). Conversely, when substation k executes the startup operation and not satisfy the SOZ constrain, $N_{k,t}^{temp}$ is bound to be smaller than the lower bound of SOZ, and needs to be adjusted to this bound, whereas the remaining substations in Sub_t^{in} need to decrease the output. Thus, find the substation with $R_S^{dec}(s_{k,t})$, and subtract N_{step} from it, namely Equation (55).

After conducting the one-step output adjustment in AM-PS for one time, update $N_{k,S}^{dec}(s_{k,t})$ by Equation (48), $N_{k,S}^{inc}(s_{k,t})$ by Equation (49), $R_S^{inc}(s_{k,t})$ by Equation (52) and $R_S^{dec}(s_{k,t})$ by Equation (54). The adjustment diagram is shown in Figure 6.

$$\begin{cases} N_{k,t}^{temp} = N_{k,S}^{min}(H_t^{gross}, s_{k,t}), \\ \quad if\ N_{k,t}^{temp} < N_{k,S}^{min}(H_t^{gross}, s_{k,t}) \\ N_{k,t}^{temp} = N_{k,S}^{max}(H_t^{gross}, s_{k,t}), \\ \quad if\ N_{k,t}^{temp} > N_{k,S}^{max}(H_t^{gross}, s_{k,t}), \end{cases} \quad k \in Sub_t^{out} \quad (51)$$

$$R_S^{inc}(s_{k,t}) = \max\{N_{k,S}^{inc}(s_{k,t}) / N_{k,S}^{max}(H_t^{gross}, s_{k,t})\}, \quad k \in Sub_t^{in} \quad (52)$$

$$N_{k,t}^{temp} = N_{k,t}^{temp} + N_{step}, \quad k\ with\ R_S^{inc}(s_{k,t}) \quad (53)$$

$$R_S^{dec}(s_{k,t}) = \max\{N_{k,S}^{dec}(s_{k,t}) / N_{k,S}^{max}(H_t^{gross}, s_{k,t})\}, \quad k \in Sub_t^{in} \quad (54)$$

$$N_{k,t}^{temp} = N_{k,t}^{temp} - N_{step}, \quad k\ with\ R_S^{dec}(s_{k,t}) \quad (55)$$

(6) If the values of $Diff_{k,t}$ s corresponding to Sub_t^{out} are all equal to zero, the AM-PS is terminated. Otherwise, the process returns to Step (1), and the switching strategy is updated to expand the range of the SOZ at substation k. Specifically, when executing the startup operation, the unit with the lowest lower bound of the SOZ has the highest priority for startup,

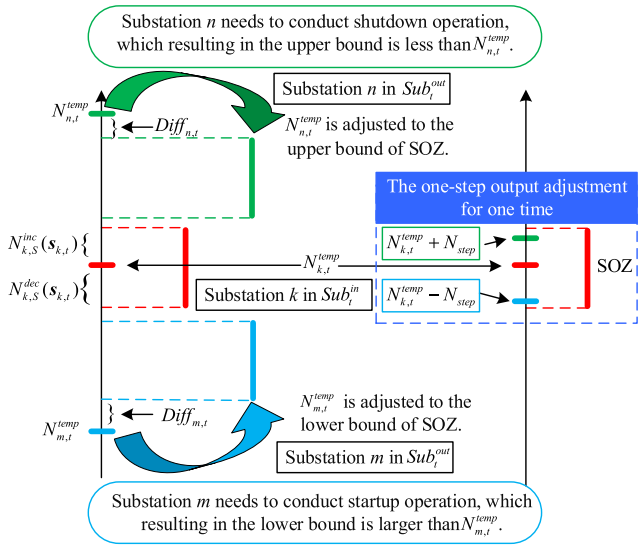

FIGURE 6. Adjustment diagram in adjustment module with practical strategies (AM-PS).

which can lower the lower bound of SOZ. Conversely, when executing the shutdown operation, the unit with the lowest upper bound of the SOZ has the highest priority for shutdown, which can raise the upper bound of SOZ.

The flowchart of AM-PS is as follows:

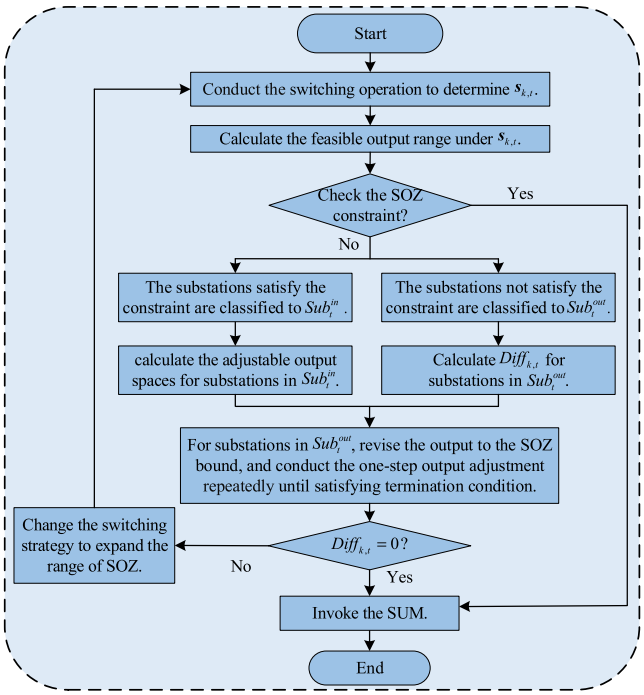

FIGURE 7. Flowchart of adjustment module with practical strategies (AM-PS).

D. OVERALL FLOW

Based on the three modules, the overall flow of the UCLD-SC is as follows; the flow chart is shown in Figure 8.

(1) Read the items of the calculation conditions, including the triple constraint sets, inflow and supply streamflow, load instructions, FWL of Gezhouba within the dispatching period, and the output and online/offline times of the units at the initial time of dispatching.

(2) Utilize $\overline{R_{flow}}$ and N_t to estimate the outflow, namely Q_{temp}.

$$Q_{temp} = \overline{R_{flow}} \times N_t + Q_t^{sup} \tag{56}$$

(3) Calculate H_t^{gross} using Equation (16), and invoke the WPSM to generate the initial output of substations.

(4) Determine the unit commitment $s_{k,t}$, and verify the SOZ constraints by Formula (46). If satisfied, invoke the SUM; then, the outflow added by the streamflow through units is calculated, namely the Q_{cal}. Otherwise, the process proceeds to Step (5).

(5) Invoke the AM-PS to adjust the output of substations; then, invoke the SUM to calculate the outflow, namely the Q_{cal}.

(6) Compare Q_{temp} with Q_{cal}. If the convergence condition $|Q_{temp} - Q_{cal}| \leq Q_{tol}$ holds, terminate the iteration of the UCLD-SC, and obtain the results of UCLD. Otherwise, $Q_{temp} = Q_{cal}$, and the process returns to Step (3).

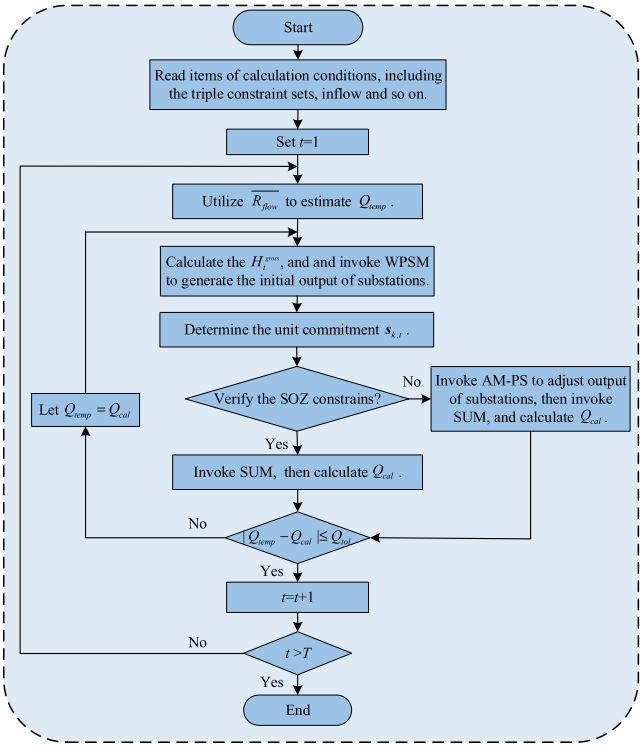

FIGURE 8. Flowchart of unit commitment and load distribution considering constraints of substations (UCLD-SC).

E. COMPARATIVE EXPERIMENTS AND EVALUATION INDEXES

To comprehensively demonstrate the effects of the RPM, comparisons and analysis will be carried out from two

aspects. The first aspect is to test computational efficiencies and outflow accuracies of RPM, which can be assisted by comparative experiments. Hence, the variable comprehensive efficiency coefficient method (VKM) [45] and the water consumption rate method (RM) [46] for their high precision and timeliness are selected to calculate the outflow as contrast experiments. The FWL process of Gezhouba was set as the actual process in three methods. The steps of contrast experiments were as follows.

(1) The items for the calculation conditions were read.

(2) According to the initial FWL, the constraints of FWL and outflow, determined the feasible range of the FWL at the end of period t, as follows:

$$V_t^L = V_{t-1} + (I_t - Q_U) \cdot \Delta t \tag{57}$$
$$Z_t^L = Z(V_t^L) \tag{58}$$
$$V_t^U = V_{t-1} + (I_t - Q_L) \cdot \Delta t \tag{59}$$
$$Z_t^U = Z(V_t^U) \tag{60}$$
$$Z_t^{Max} = \min\{Z_t^U, Z_{t-1} + Z_{rise}^{bear}, Z_U\} \tag{61}$$
$$Z_t^{Min} = \max\{Z_t^L, Z_{t-1} - Z_{drop}^{bear}, Z_L\} \tag{62}$$

(3) Discretize $[Z_t^{Min}, Z_t^{Max}]$ by Z_{step} to obtain $\mathbf{Z}_t$. Iterate through $\mathbf{Z}_t$, and find Z_t^H. For each FWL in $\mathbf{Z}_t$, Q_t and H_t^{gross} are calculated by Equation (3) and (16). For the VKM, utilize Equation (63) calculate K, and utilize Equation (64) to estimate outflow. For the RM, utilize Equation (65) to calculate R_{flow}, and utilize Equation (66) to estimate outflow.

$$K = K(H_t^{gross}) \tag{63}$$
$$Q_t = \frac{N_t}{KH_t^{gross}} + Q_t^{sup} \tag{64}$$
$$R_{flow} = R_{flow}(H_t^{gross}) \tag{65}$$
$$Q_t = R_{flow} \times N_t + Q_t^{sup} \tag{66}$$

(4) Narrow the FWL range, and then calculate the outflow using the dichotomy method. If the interval $[Z_t^H, Z_t^{Max}]$ contains the output less than N_t, then the FWL range $[Z_t^H, Z_t^{Max}]$ is appropriate. Otherwise, the FWL range $[Z_t^{Min}, Z_t^H]$ is appropriate. Owing to the nonlinearity, a decrease in the FWL does not necessarily lead to an increase in output. Therefore, narrowing the range of the FWL can make the calculation convergent. The terminal condition of the dichotomy method is that N_{tol} is within the acceptable error.

In this study, the load instructions were set for the actual process. The TGHS has been running steadily for many years and has accumulated significant dispatching experience, in which the hydro units often operate under suboptimal conditions. Hence, the high accuracy of outflow means that the calculated streamflow is close to the actual value. The pivotal evaluation indexes [47] are listed as follows:

$$ACT = \frac{1}{G}\sum_{g=1}^{G} CT_g \tag{67}$$
$$MAE = \frac{1}{T}\sum_{t=1}^{T}\left|Q_t^{act} - Q_t^{cal}\right| \tag{68}$$

TABLE 1. Partial results for Optimal Load Allocation Table-Whole Plant (OLAT-WP) with a gross water head value equal to 80 m.

H_{gross}	N_{total}	Q_{opt}	H_{gross}	N_{total}	Q_{opt}
80	2179	32139	80	2157	31073
80	2178	32071	80	2156	31067
80	2177	32002	80	2155	31010
80	2176	31934	80	2154	31004
80	2175	31867	80	2153	30975
80	2174	31800	80	2152	30941
80	2173	31733	80	2151	30936
80	2172	31666	80	2150	30907
80	2171	31600	80	2149	30872
80	2170	31533	80	2148	30867
80	2169	31466	80	2147	30838
80	2168	31464	80	2146	30804
80	2167	31397	80	2145	30798
80	2166	31396	80	2144	30770
80	2165	31329	80	2143	30735
80	2164	31329	80	2142	30731
80	2163	31262	80	2141	30701
80	2162	31260	80	2140	30668
80	2161	31199	80	2139	30663
80	2160	31193	80	2138	30634
80	2159	31136	80	2137	30600
80	2158	31130	···	···	···

The units of parameters are listed in APPENDIX.

$$RMAE = \frac{MAE}{\frac{1}{T}\sum_{t=1}^{T} Q_t^{act}} \tag{69}$$
$$MD = \max\{\left|Z_t^{cal} - Z_t^{act}\right|\}, \quad t = 1, 2, \cdots, T \tag{70}$$

The second aspect is to analyze the rationality and practicability of UCLD results from RPM. However, there are currently no relevant methods for solving the UCLD problem considering constrains of substations. Hence, some insight discussions, such as the operation efficiency of units, the on-off situations of units, the situations of crossing between SOZ and FOZ, and load transfer situations of substations [47], are made based on the UCLD results from RPM.

V. CASE STUDY

A. PARAMETER SETTING

The uniform parameters of the UCLD-SC were first introduced in different cases. The length of the dispatching period was set to one day. The time scale was 2 h, as the streamflow was calculated in the TGCDCC every 2 h [6]. The values of Z_{rise}^{bear} and Z_{drop}^{bear} for restricting the fluctuation amplitude of the FWL were set to 1 m and 0.6 m, respectively. The lower and upper bounds of FWL are 145 m and 175 m. While the lower and upper bounds of outflow are 6000 m^3/s and 98800 m^3/s, respectively. For all substations, the value of Num_k^{min} was set to one. For all units, T_i^{up} and T_i^{down} were set to 4 h. The N_{step} in the WPSM and AM-PS was set to 10 MW. The N_{tol} in the dichotomy method was set to 1MW. Z_{step} was set to 0.01 m, as each change of 0.01 m in the FWL of the TGHS would lead to a change in the outflow of up to approximately 1000 m^3/s with a 2-h scale. Q_{tol} was set to 50 m^3/s to ensure the accuracy of H_t^{gross}. The results from the OLAT-WP are shown in TABLE 1.

TABLE 2. Key information of the typical scenarios in 2021.

Scenario	Number	Bus	N_{max}^{grid}	Num_{max}	Peaking	Repairing
January 12	5	L-off/R-on	17550	25	5760/25.6%	7, 14, 24, 25
April 1	4	L-on/R-on	11950	17	4230/18.8%	6, 7, 23–25, 29, 33

In the above, Number is the total number of substations in the corresponding scenario. L-off indicates that the bus connection switch of the left bank is separate. The value before / is the amplitude of the peak regulation, whereas the latter is the rate between the peak regulation amplitude and installed capacity of the TGHS. Repairing lists the units in the repair status. The unit of peaking amplitude is MW, while the units of other parameters are listed in APPENDIX.

In addition, the cases were selected from 2021, as only the actual operation data, including the repair plans for the units and on-off states of the bus connection switches from January 1 to April 7 in 2021 were available. Utilizing the actual data during the non-abandoning water season from 2018 to 2020, the mean of water consumption rate was calculated as 11.47 m^3/(skw). The relationship curves, including $K \sim H_t^{gross}$, $R_{flow} \sim H_t^{gross}$ and $\Delta Z_t \sim Q_t$, were showed as follows:

$$K = -1.052 \times 10^{-3} H_t^{gross^2} + 0.2105 \times H_t^{gross} - 1.36 \quad (71)$$

$$R_{flow} = 2.917 \times 10^{-3} H_t^{gross^2} - 0.6951 \times H_t^{gross} + 51.23 \quad (72)$$

$$\Delta Z_t = 2.2 \times 10^{-9} \times Q_t^2 + 3.1 \times 10^{-5} \times Q_t - 0.14 \quad (73)$$

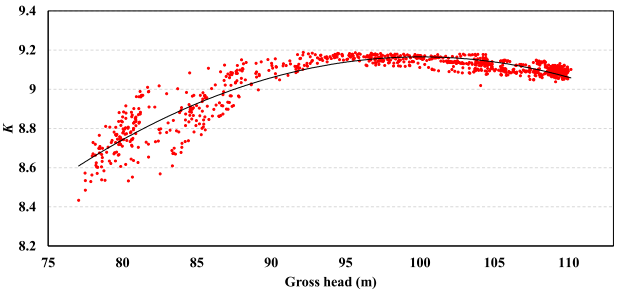

FIGURE 9. Scatter plot showing the relationship between comprehensive efficiency coefficient and gross head.

B. RESULTS AND DISCUSSION

In 2021, the bus connection switch of the left bank was separated from January 1 to January 20, and was closed from January 21 to April 7. However, the right one was always closed. Therefore, a typical scenario was selected as the simulation case in each period, namely January 12 and April 1, respectively. A bimodal operation condition with a large peak modulation amplitude was selected as the typical scenario. This condition exhibited a multi-stage load fluctuation, and the aftereffects of the tail water level were stronger, thereby providing a good test of the effects of the RPM. In addition, the main function of the power substation

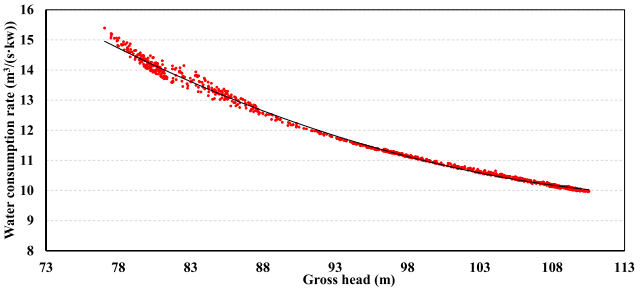

FIGURE 10. Scatter plot showing the relationship between water consumption rate and gross head.

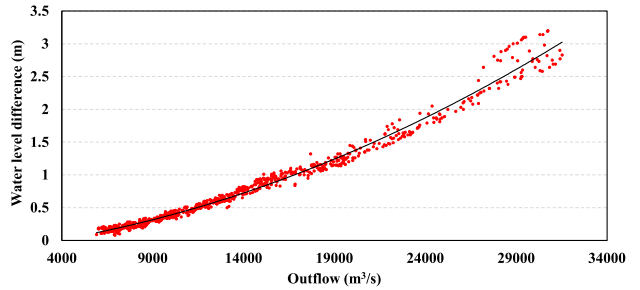

FIGURE 11. Scatter plot showing the relationship between water level difference and outflow.

is to supply power to the TGHS. In daily dispatching, the power substation seldom participated in optimizing the dispatching for the UCLD-SC. Therefore, we set the condition of the power substation as the actual condition. Under the parameters mentioned in Section V-A, the three methods were utilized to calculate the outflow process. While the RPM are utilized to solve the UCLD-SC with triple constraint sets. The key information for the two cases is presented in Table 2.

In the above, Number is the total number of substations in the corresponding scenario. L-off indicates that the bus connection switch of the left bank is separate. The value before / is the amplitude of the peak regulation, whereas the latter is the rate between the peak regulation amplitude and installed capacity of the TGHS. Repairing lists the units in the repair status. The unit of peaking amplitude is MW, while the units of other parameters are listed in APPENDIX.

First, evaluation indexes of the two scenarios are listed in TABLE 3. Overall, the effects of VKM and RM are almost the same. For the perspective of timeliness, the cases are conducted on a personal computer with a 1.6 GHz processor and 8 GB of RAM. For each case, identical calculations are performed ten times and the average time consumption of the three methods is less than 1 s, indicating that looking up the OLAT-WP to determine the load distribution is efficient to solve the UCLD problem with 34 units. Comparing with VKM and RM which not involving units, the calculation efficiency of RPM not decreases significantly.

For the perspective of accuracy, even though the *MAE* of RPM is slightly larger than that of the VKM and RM, its *MAE* can be limited within 100 m^3/s, and its *RMAE* can still be limited within 1%. The differences between the simulated and actual flows are shown in Figure 12 and 13. Seen from the figures, the simulation outflow tracks the trend of the actual process well. Even in periods with large fluctuations in output and outflow, the outflow error does not increase significantly, reflecting the high robustness of RPM. High accuracy in simulating outflow makes the FWL deviation controlled within 0.1 m throughout the entire period. In addition, it should not be ignored that most of the streamflow as simulated by the VKM and RM is less than the actual one. The actual streamflow through the units usually falls within an excellent allocation scheme. Hence, the reliability of VKM and RM is questionable. While, the RPM can consider the unit commitment and provide more specific dispatching advice for hydropower stations.

TABLE 3. Indexes of the two scenarios with different methods.

Sch/Ind	*ACT*	*MAE*	*RMAE*	*MD*
Jan-12-RPM	<1	53	0.56%	<0.1
Jan-12-VKM	<1	25	0.26%	<0.1
Jan-12-RM	<1	29	0.31%	<0.1
Apr-1-RPM	<1	85	0.87%	<0.1
Apr-1-VKM	<1	19	0.19%	<0.1
Apr-1-RM	<1	24	0.25%	<0.1

In the above, Sch and Ind are the abbreviations of schemes and indexes, respectively. Jan-12-RPM mean the RPM in January 12. The units of indexes are listed in APPENDIX.

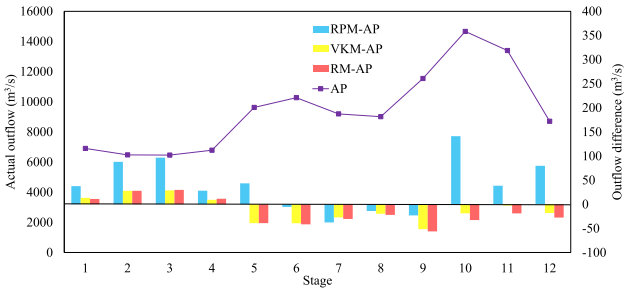

FIGURE 12. Difference between simulation outflow and actual process (AP) on January 12.

Next, analysis comes to rationality and practicability. For the operation efficiency, TABLEs 4 and 5 show the

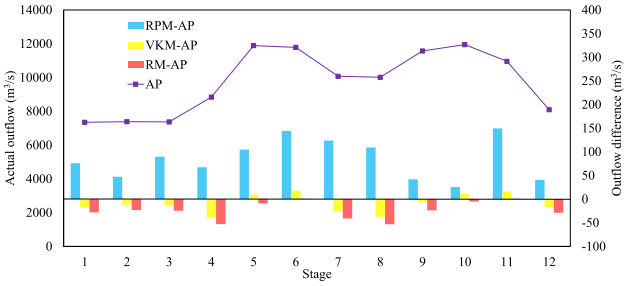

FIGURE 13. Difference between simulation outflow and AP on April 1.

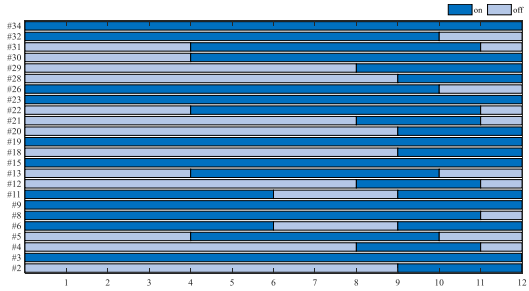

FIGURE 14. Scheme for starting up and shutting down units on January 12.

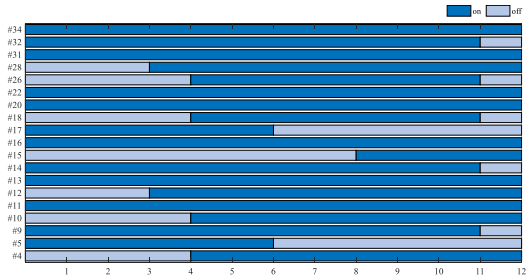

FIGURE 15. Scheme for starting up and shutting down units on April 1.

output processes of units. Except for the units in the power substation, no operating unit undertakes an output of less than 490 MW. (The installed capacity of units in the power substation is only 50 MW.) By statistics, the indicators Num_{max} on January 12 and April 1 are equal to 24 and 18, respectively. Though the Num_{max} on April 1 is slightly larger than the given one in TABLE 2, the outputs of units are determined by consulting the OLAT-WP, the load distribution within each substation is optimal. Hence, the operational efficiency of units can be guaranteed, not to mention this constraint (i.e., Formula (12)) is a soft constraint.

For the on-off situations, Figures 14 and 15 show the scheme for starting up and shutting down units. During the entire period, there is no frequent switching for the units, and the on-line/off-line time is larger than 4 h. The conversions of units in the on-off state are based on the unit combination in the previous period, and make full use of the adjustable output spaces (utilized in WPSM and AM-PS) to cope with the load fluctuations. Hence, the soft constraint limiting the switching of units in Formula (19) can be satisfied in general.

TABLE 4. Load distribution determined by Refined and Practical Method (RPM) of TGHS on January 12 in 2021.

Stage	1	2	3	4	5	6	7	8	9	10	11	12
#2	0.0	0.0	0.0	0.0	0.0	0.0	0.0	0.0	0.0	63.5	67.9	69.9
#3	67.5	66.8	66.5	66.7	64.8	66.8	70.0	70.0	69.9	63.5	67.9	69.1
#4	0.0	0.0	0.0	0.0	0.0	0.0	0.0	0.0	68.9	58.5	62.9	0.0
#5	0.0	0.0	0.0	0.0	59.8	66.8	70.0	68.0	67.9	58.5	0.0	0.0
#6	62.5	61.8	61.5	66.7	59.8	61.8	0.0	0.0	0.0	58.5	62.9	67.9
#8	63.3	64.8	65.4	66.7	63.1	66.8	70.0	69.0	69.9	63.5	67.9	0.0
#9	69.4	67.3	67.3	66.8	61.7	67.3	70.0	69.0	67.7	62.6	70.0	70.0
#11	68.6	62.3	62.3	66.8	61.7	67.3	0.0	0.0	0.0	62.6	70.0	70.0
#12	0.0	0.0	0.0	0.0	0.0	0.0	0.0	0.0	67.7	62.6	70.0	0.0
#13	0.0	0.0	0.0	0.0	61.7	62.3	70.0	68.0	62.7	62.6	0.0	0.0
#15	67.8	60.3	60.3	67.5	61.2	62.3	67.6	62.8	62.3	64.5	67.6	62.5
#18	0.0	0.0	0.0	0.0	0.0	0.0	0.0	0.0	0.0	64.5	67.6	62.5
#19	68.8	60.3	60.3	67.5	61.2	67.3	67.6	67.8	67.3	59.5	67.6	56.4
#20	0.0	0.0	0.0	0.0	0.0	0.0	0.0	0.0	0.0	59.5	67.6	56.4
#21	0.0	0.0	0.0	0.0	0.0	0.0	0.0	0.0	67.3	59.5	62.6	0.0
#22	0.0	0.0	0.0	0.0	61.2	67.3	67.6	67.8	67.3	59.5	62.6	0.0
#23	69.8	63.3	63.3	65.5	64.2	65.3	65.6	65.8	65.3	64.5	66.6	62.1
#26	69.8	63.3	63.3	65.5	64.2	65.3	65.6	65.8	65.3	54.5	0.0	0.0
#28	0.0	0.0	0.0	0.0	0.0	0.0	0.0	0.0	0.0	63.0	67.8	59.6
#29	0.0	0.0	0.0	0.0	0.0	0.0	0.0	0.0	63.0	63.0	69.8	62.6
#30	0.0	0.0	0.0	0.0	67.7	68.0	68.9	69.9	58.0	58.0	68.8	57.6
#31	0.0	0.0	0.0	0.0	57.7	66.0	65.9	63.3	58.0	58.0	66.9	0.0
#32	57.1	57.3	57.4	57.5	57.7	63.0	65.9	60.5	58.0	58.0	0.0	0.0
#34	5.0	5.0	5.0	5.0	5.0	5.0	5.0	5.0	5.0	5.0	5.0	5.0

Here, #2 denotes unit 2 in TGHS. If a unit does not appear in the table, it is always in the off state. Units with the same background color are in the same substation. The unit of output is 10 MW in this table.

TABLE 5. Load distribution determined by RPM of TGHS on April 1 in 2021.

Stage	1	2	3	4	5	6	7	8	9	10	11	12
#4	0.0	0.0	0.0	0.0	63.3	63.2	61.8	62.0	70.0	70.0	64.3	69.9
#5	59.2	59.4	59.6	63.3	62.1	61.4	0.0	0.0	0.0	0.0	0.0	0.0
#9	56.6	56.2	55.6	59.1	61.3	62.6	60.5	59.6	70.0	70.0	64.3	0.0
#10	0.0	0.0	0.0	0.0	63.3	63.2	61.8	62.0	70.0	70.0	64.3	67.9
#11	59.2	59.4	59.6	63.3	63.3	63.2	61.8	62.0	70.0	70.0	64.3	67.9
#12	0.0	0.0	0.0	63.3	63.3	63.2	61.8	62.0	70.0	70.0	64.3	67.9
#13	59.2	59.4	59.6	63.3	63.3	63.2	61.8	62.0	70.0	70.0	64.3	67.9
#14	57.2	57.4	57.6	61.3	63.3	63.2	61.8	62.0	70.0	70.0	64.3	0.0
#15	0.0	0.0	0.0	0.0	0.0	0.0	0.0	0.0	60.1	64.8	61.9	63.0
#16	65.8	66.1	66.4	67.2	62.9	63.1	64.4	63.2	60.1	64.8	61.9	63.0
#17	63.3	63.0	62.4	67.2	62.9	63.1	0.0	0.0	0.0	0.0	0.0	0.0
#18	0.0	0.0	0.0	0.0	62.9	63.1	63.6	63.2	60.1	65.7	61.9	0.0
#20	66.8	66.9	66.8	67.8	64.1	64.8	67.1	64.2	61.2	67.3	63.9	65.8
#22	66.8	66.9	66.8	67.5	64.1	64.8	67.1	66.6	61.2	67.3	63.9	65.8
#26	0.0	0.0	0.0	0.0	61.1	59.1	61.5	62.0	58.7	65.3	56.9	0.0
#28	0.0	0.0	0.0	57.1	70.0	61.2	56.7	56.8	70.0	70.0	61.0	70.0
#31	63.0	64.1	64.9	55.1	70.0	70.0	54.7	54.8	70.0	70.0	61.0	70.0
#32	55.0	57.7	56.9	54.1	70.0	67.7	53.7	53.8	70.0	70.0	61.0	0.0
#34	3.8	3.8	3.8	3.8	3.8	3.8	3.8	3.8	3.8	3.8	3.8	3.8

The unit of output is 10 MW in this table.

These practical strategies reduce the unnecessary crossings between SOZ and FOZ, improving the safety of the power grid and hydro units.

For the load transfer situations, Figure 16 and 17 show the output trend of substations following load instructions. (Here, the output of the power substation is located at the bottom, and it is too small to be visible in the figures.) The one-step output adjustments in WPSM and AM-PS all take the installed capacity difference of substations into account. Hence, there is no load transfer with a large amplitude between substations, and all substations can cooperate with each other to share the fluctuations of the load instructions. All substations ensure that at least one unit is in operation, thereby preventing some substations from undertaking an empty load.

When solved the UCLD problem, the three categories of methods mentioned in Introduction not consider the SOZ constrains of substations. Hence, it is quite possible that in some peak regulation conditions, the UCLD results from them do not meet the actual needs of power generation

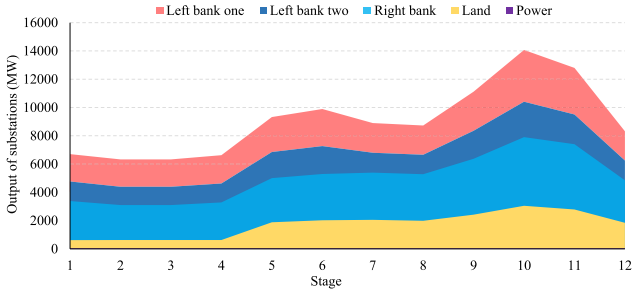

FIGURE 16. The output processes of substations on January 12.

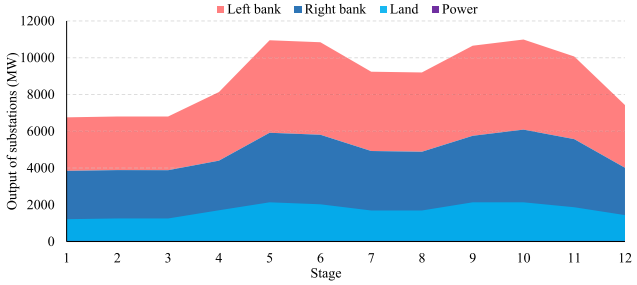

FIGURE 17. The output processes of substations on April 1.

enterprises. While, the RPM successfully solves the UCLD-SC problem, and combine calculation efficiencies and accuracies. This is the outstanding advantages of RPM.

VI. CONCLUSION

In this study, substation constraints are considered in the unit commitment and load distribution of hydropower stations for the first time. The complex constraints in the UCLD-SC are classified into three constraint sets, namely, CS-HSL, CS-SL, and CS-UL. A refined and practical method for solving the UCLD-SC is proposed, and contains three submodules. Among them, the WPSM and AM-PS jointly guarantees the output of substations following load fluctuations, and determine the reasonable unit commitment. While, the SUM guarantees the calculation timeliness, load distribution scheme and efficiencies of units. Owing to its representativeness and complexity, the TGHS is selected to verify that the RPM is a highly time-efficient and adaptable method for the UCLD-SC, and is of vital importance for large hydropower stations to execute critical dispatching, such as arranging unit commitments and forecasting the FWL process of the next day. The main research contributions of this study are as follows.

(1) A unit commitment and load distribution model considering the constraints of substations is abstracted and established. Subsequently, a refined method with practical strategies (RPM) for solving the UCLD-SC is proposed for the first time.

(2) The RPM can guarantee the operation efficiency of units, avoid units frequently crossing between SOZ and FOZ, and reasonably arrange substation output to jointly undertake load fluctuations, namely the UCLD scheme by RPM is with high rationality and practicability.

(3) The calculation timeliness and accuracy of RPM are almost identical to that of VKM and RM. The relative *MAE* of the simulation outflow can be controlled within 1%. The RPM involving the unit level can be treated as a trustworthy method for forecasting the FWL and outflow processes.

The RPM has good timeliness and rationality, but there remain some drawbacks. In particular, the SUM can only guarantee the optimal allocation of the streamflow within each substation, and the AM-PS does not consider the efficiency of the units from the whole plant, which resulting in a violation of the first soft constraint on April 1. Thus, improving the strategies in the AM-PS requires further study.

APPENDIX
NOMENCLATURE

SETS AND INDICES

T, t	Set and index of time periods.
I, i	Set and index of units from the perspectives of the whole plant.
J, j	Set and index of units from the perspectives of substations.
K, k	Set and index of substations.
FSS	Set, namely substations that satisfy the SOZ constraint under H_t^{gross} and $\boldsymbol{s}_{k,t-1}$.
Sub_t^{in}	Set, namely substations satisfying the SOZ constraint under $\boldsymbol{s}_{k,t}$.
Sub_t^{out}	Set, namely substations not satisfying the SOZ constraint under $\boldsymbol{s}_{k,t}$.
g	Index of repeated experiments.

CONSTANTS

Δt	Length of one period [s].
T_i^{up}	Shortest time in the on state of unit i [h].
T_i^{down}	Shortest time in the off state of unit i [h].
Z_L	Lower bounds of forebay water level [m].
Z_U	Upper bounds of forebay water level [m].
Z_{rise}^{bear}	Bearable rise in forebay water level [m].
Z_{drop}^{bear}	Bearable drop in forebay water level [m].
H_L	Lower bound of gross water head [m].
Z_{step}	Discrete step of water level [m].
H_U	Upper bound of gross water head [m].
Q_L	Lower bound of outflow [m^3/s].
Q_U	Upper bound of outflow [m^3/s].
Q_t	Outflow at period t [m^3/s].
Q_t^{act}	Actual outflow at period t [m^3/s].
V_{t-1}	Initial water volume of the hydropower station at period t [m^3].
V_t^L	Water volume corresponding to Q_U [m^3].
V_t^U	Water volume corresponding to Q_L [m^3].
$\boldsymbol{N}$	Load instruction sequence of the whole plant [MW].
N_t	Output for the entire plant at period t [MW].
$N_{i,t}$	Output of unit i at period t from the perspectives of the whole plant [MW].

$N_{k,t}^{ini}$ Initial output of the substations at the beginning of period t [MW].
$N_{k,t}^{temp}$ Temporary output of substations at period t [MW].
$N_{k,t}$ Output of substation k in period t [MW].
$N_{k,j,t}$ Output of unit j at period t and substation k [MW].
ΔN_t Load fluctuation of the whole plant at period t [MW].
N_k^{diff} Output difference between N_k^{max} and $N_{k,t}^{ini}$ [MW].
N_k^{max} Maximum output of substations for units in the non-repairing state at period t [MW].
$N_{k,j}^{max}$ Maximum output of unit j at substation k [MW].
$N_{k,j}^{exp}$ Expected output of unit j at substation k [MW].
$N_{k,pre}^{max}$ Maximum output at substation k under $\boldsymbol{s}_{k,t-1}$ [MW].
$N_{k,pre}^{min}$ Minimum output of substation k under $\boldsymbol{s}_{k,t-1}$ [MW].
N_{step} Discrete step of output, and positive number [MW]. In Section IV-A, if $|\Delta N_t| > N_{step}$, N_{step} equals a constant but equals $|\Delta N_t|$ otherwise. In Section IV-C, if $Diff_{k,t} > N_{step}$, N_{step} equals a constant but equals $Diff_{k,t}$ otherwise.
Q_{tol} Error tolerance value of outflow [m^3/s].
N_L Lower bound of output [MW].
N_U Upper bound of output [MW].
N_{tol} Absolute deviation between the calculated output and load instruction [MW].
N_{max}^{grid} Maximum output of the entire plant [MW].
$N_{k,j}^{rated}$ Rated output of unit j at substation k [MW].
Num_k^{min} Minimum operational number of units at substation k.
$J(k)$ Total unit number of substation k.
Num_{max} Maximum operational number of units.
S_{on} Bus connection switching is in closed state.
S_{off} Bus connection switching is in separate state.
Re_{on} A unit is in the non-repairing state.
Re_{off} A unit is in the repairing state.
G Total times of repeated experiments.

VARIABLES

CT_g Calculation time of the gth experiment [s].
$T_{i,t}^{on}$ Durations of the on-line state of unit i until period t [h].
$T_{i,t}^{off}$ Durations of the off-line state of unit i until period t [h].
$\boldsymbol{Z}_t$ Sequence of discrete forebay water level [m].
Z_t Forebay water level at period t [m].
Z_t^H Forebay water level with the maximum output among $\boldsymbol{Z}_t$ [m].
Z_t^{tail} Tailwater level of the hydropower station [m].
Z_t^L Forebay water level corresponding to V_t^L [m].
Z_t^U Forebay water level corresponding to V_t^U [m].
Z_t^{gzb} Mean value of the forebay water level of Gezhouba [m].
Z_t^{act} Actual forebay water level at period t [m].
Z_t^{cal} Calculated forebay water level by different methods at period t [m].
Z_t^{Max} Maximum forebay water level at the end of period t [m].
Z_t^{Min} Minimum forebay water level at the end of period t [m].
$N_{k,j}^{P}$ Output of unit j at substation k and row P [MW].
$N_{k,S}^{max}$ Maximum output bound under $\boldsymbol{s}_{k,t}$ [MW].
$N_{k,S}^{min}$ Minimum output bound under $\boldsymbol{s}_{k,t}$ [MW].
N_k^{dec} Adjustable space for decreasing output [MW].
N_k^{inc} Adjustable space for increasing output [MW].
ΔN_t^{sum} Total output in one-step adjustments [MW].
$Diff_{k,t}$ Nearest distance between $N_{k,t}^{temp}$ and the bounds of the SOZ [MW].
$N_{k,S}^{inc}$ Adjustable output space between $N_{k,S}^{max}$ and $N_{k,t}^{temp}$, [MW].
$N_{k,S}^{dec}$ Adjustable output space between $N_{k,t}^{temp}$ and $N_{k,S}^{min}$,[MW].
N_{total} Output of the entire plant in TABLE 1 [10 MW].
$\overline{R_{flow}}$ Mean of the water consumption rate in the recent three years [m^3/(skw)].
$u_{i,t}$ Binary variable that equals 1 if unit i at period t is on but equals 0 otherwise.
$u_{k,j,t}$ Binary variable that equals 1 if unit j at period t and substation k is on but equals 0 otherwise.
$s_{k,j,t-1}$ On-off state of unit j at substation k and period t-1.
$\boldsymbol{s}_{k,t-1}$ On-off state vector of substation k in period t-1.
S_L Bus connection switching state of the left bank.
S_R Bus connection switching state of the right bank.
Re_i Repairing state of unit i.
$Re_{k,j}$ Repairing state of unit j of substation k.
R^{dec} Maximum rate between N_k^{dec} and $N_{k,pre}^{max}$.
R^{inc} Maximum rate between N_k^{inc} and $N_{k,pre}^{max}$.
R_{max}^{diff} Maximum rate between N_k^{diff} and N_k^{max}.
R_{min}^{diff} Minimum rate between N_k^{diff} and N_k^{max}.
R_S^{inc} Maximum rate between $N_{k,S}^{inc}$ and $N_{k,S}^{max}$.
R_S^{dec} Maximum rate between $N_{k,S}^{dec}$ and $N_{k,S}^{max}$.
M Total times of executions of the one-step adjustment.

INDEXES

ACT Average calculation time of experiments [s].
ΔZ_t Water level difference between Z_t^{tail} and Z_t^{gzb} [m].
$H_{i,t}$ Water head of unit i at period t [m].

H_t^{gross}	Gross water head of the hydropower station at period t [m].
H_{gross}	Gross water head in TABLE 1 [m].
I_t	Inflow at period t [m^3/s].
Q_{opt}	Optimal generation streamflow through the units under H_{gross} and N_{total} [m^3/s].
Q_{temp}	Estimated outflow by the mean of the water consumption rate at period t [m^3/s].
Q_{cal}	Calculate outflow added by the streamflow through units in Section IV-D [m^3/s].
$Q(\boldsymbol{N})$	Approximate optimal outflow when the load sequence is $\boldsymbol{N}$ [m^3/s].
Q_t^{cal}	Calculate outflow by different methods at period t [m^3/s].
Q_t^{sup}	Supply streamflow at period t, including the streamflow through the ship locks and so on [m^3/s].
$Q_{i,t}$	Power generation streamflow through unit i [m^3/s].
MAE	Mean absolute outflow error between Q_t^{act} and Q_t^{cal} [m^3/s].
$RMAE$	Rate between MAE and the mean of the actual outflow.
MD	Maximum forebay water level difference throughout the entire period [m].

FUNCTIONS

$\Delta Z(\cdot)$	Water level difference as a function of its outflow.
$\tilde{\min}(\cdot)$	Approximately minimum function.
$L_{k,j}(\cdot)$	Lower bound of stable operation zone of unit j at substation k as a function of its gross water head.
$U_{k,j}(\cdot)$	Upper bound of stable operation zone of unit j at substation k as a function of its gross water head.
$Z(\cdot)$	Forebay water level as a function of its water volume.
$R_{flow}(\cdot)$	Water consumption rate as a function of its gross water head.
$K(\cdot)$	Comprehensive efficiency coefficient as a function of its gross water head.

REFERENCES

[1] L. Wu and Q. Zhu, "Impacts of the carbon emission trading system on China's carbon emission peak: A new data-driven approach," *Natural Hazards*, vol. 107, no. 3, pp. 2487–2515, Jul. 2021.

[2] R. Wang, Q. Wang, and S. Yao, "Evaluation and difference analysis of regional energy efficiency in China under the carbon neutrality targets: Insights from DEA and Theil models," *J. Environ. Manage.*, vol. 293, Sep. 2021, Art. no. 112958.

[3] W. Zhou, C. Lou, Z. Li, L. Lu, and H. Yang, "Current status of research on optimum sizing of stand-alone hybrid solar–wind power generation systems," *Appl. Energy*, vol. 87, no. 2, pp. 380–389, Feb. 2010.

[4] M. A. Abbaszadeh, M. J. Ghourichaei, and F. Mohammadkhani, "Thermo-economic feasibility of a hybrid wind turbine/PV/gas generator energy system for application in a residential complex in Tehran, Iran," *Environ. Prog. Sustain. Energy*, vol. 39, no. 4, Jul. 2020, Art. no. e13396.

[5] M. Basu, "Dynamic economic dispatch with demand-side management incorporating renewable energy sources and pumped hydroelectric energy storage," *Electr. Eng.*, vol. 101, no. 3, pp. 877–893, Sep. 2019.

[6] Y. Shang, Y. Xu, L. Shang, Q. Fan, Y. Wang, and Z. Liu, "A method of direct, real-time forecasting of downstream water levels via hydropower station reregulation: A case study from Gezhouba Hydropower Plant, China," *J. Hydrol.*, vol. 573, pp. 895–907, Jun. 2019.

[7] Y. Zhang, C. Ma, Y. Yang, X. Pang, L. Liu, and J. Lian, "Study on short-term optimal operation of cascade hydro-photovoltaic hybrid systems," *Appl. Energy*, vol. 291, Jun. 2021, Art. no. 116828.

[8] L. Wang, B. Wang, P. Zhang, M. Liu, and C. Li, "Study on optimization of the short-term operation of cascade hydropower stations by considering output error," *J. Hydrol.*, vol. 549, pp. 326–339, Jun. 2017.

[9] Z. Yang, K. Yang, L. Su, and H. Hu, "The short-term economical operation problem for hydropower station using chaotic normal cloud model based discrete shuffled frog leaping algorithm," *Water Resour. Manage.*, vol. 34, no. 3, pp. 905–927, Feb. 2020.

[10] C.-T. Cheng, S.-L. Liao, Z.-T. Tang, and M.-Y. Zhao, "Comparison of particle swarm optimization and dynamic programming for large scale hydro unit load dispatch," *Energy Convers. Manage.*, vol. 50, no. 12, pp. 3007–3014, Dec. 2009.

[11] T. Ohishi, E. Santos, A. Arce, M. Kadowaki, M. Cicogna, and S. Soares, "Comparison of two heuristic approaches to hydro unit commitment," in *Proc. IEEE Russia Power Tech*, Jun. 2005, pp. 1–7.

[12] C.-P. Cheng, C.-W. Liu, and C.-C. Liu, "Unit commitment by Lagrangian relaxation and genetic algorithms," *IEEE Trans. Power Syst.*, vol. 15, no. 2, pp. 707–714, May 2000.

[13] J. Zheng, M. Liu, W. Lu, M. Xie, and J. Zhu, "Extended ADMMs for RPO of large-scale power systems with discrete controls," *IET Gener., Transmiss. Distrib.*, vol. 12, no. 11, pp. 2624–2632, Jun. 2018.

[14] L. S. M. Guedes, P. de Mendonça Maia, A. C. Lisboa, D. A. G. Vieira, and R. R. Saldanha, "A unit commitment algorithm and a compact MILP model for short-term hydro-power generation scheduling," *IEEE Trans. Power Syst.*, vol. 32, no. 5, pp. 3381–3390, Sep. 2017.

[15] Z.-K. Feng, W.-J. Niu, W.-C. Wang, J.-Z. Zhou, and C.-T. Cheng, "A mixed integer linear programming model for unit commitment of thermal plants with peak shaving operation aspect in regional power grid lack of flexible hydropower energy," *Energy*, vol. 175, pp. 618–629, May 2019.

[16] Y. Shang, S. Lu, J. Gong, R. Liu, X. Li, and Q. Fan, "Improved genetic algorithm for economic load dispatch in hydropower plants and comprehensive performance comparison with dynamic programming method," *J. Hydrol.*, vol. 554, pp. 306–316, Nov. 2017.

[17] P. Lu, J. Zhou, C. Wang, Q. Qiao, and M. Li, "Short-term hydro generation scheduling of Xiluodu and Xiangjiaba cascade hydropower stations using improved binary-real coded bee colony optimization algorithm," *Energy Convers. Manage.*, vol. 91, pp. 19–31, Feb. 2015.

[18] R. Taktak and C. D'Ambrosio, "An overview on mathematical programming approaches for the deterministic unit commitment problem in hydro valleys," *Energy Syst.*, vol. 8, no. 1, pp. 57–79, Feb. 2017.

[19] X. Li, T. Li, J. Wei, G. Wang, and W. W.-G. Yeh, "Hydro unit commitment via mixed integer linear programming: A case study of the three Gorges project, China," *IEEE Trans. Power Syst.*, vol. 29, no. 3, pp. 1232–1241, May 2014.

[20] J. Chuanwen and E. Bompard, "A self-adaptive chaotic particle swarm algorithm for short term hydroelectric system scheduling in deregulated environment," *Energy Convers. Manage.*, vol. 46, no. 17, pp. 2689–2696, Oct. 2005.

[21] D. Santra, K. Sarker, A. Mukherjee, and A. Mondal, "Hybrid PSO-ACO technique to solve multi-constraint economic load dispatch problems for 6-generator system," *Int. J. Comput. Appl.*, vol. 38, nos. 2–3, pp. 96–115, Jul. 2016.

[22] M. R. Jalali, A. Afshar, and M. A. Mariño, "Multi-colony ant algorithm for continuous multi-reservoir operation optimization problem," *Water Resour. Manage.*, vol. 21, no. 9, pp. 1429–1447, Aug. 2007.

[23] C. Wang, J. Zhou, P. Lu, and L. Yuan, "Long-term scheduling of large cascade hydropower stations in Jinsha river, China," *Energy Convers. Manage.*, vol. 90, pp. 476–487, Jan. 2015.

[24] A. Y. Abdelaziz, M. A. El-Sharkawy, M. A. Attia, and B. K. Panigrahi, "Genetic algorithm based approach for optimal allocation of TCSC for power system loadability enhancement," in *Swarm, Evolutionary, and Memetic Computing* (Lecture Notes in Computer Science: Lecture Notes in Artificial Intelligence and Lecture Notes in Bioinformatics), vol. 7677. Berlin, Germany: Springer, 2012, pp. 548–557.

[25] O. Hınçal, A. B. Altan-Sakarya, and A. M. Ger, "Optimization of multireservoir systems by genetic algorithm," *Water Resour. Manage.*, vol. 25, no. 5, pp. 1465–1487, Mar. 2011.
[26] N. Sinha, R. Chakrabarti, and P. K. Chattopadhyay, "Evolutionary programming techniques for economic load dispatch," *IEEE Trans. Evol. Comput.*, vol. 7, no. 1, pp. 83–94, Feb. 2003.
[27] P. Somasundaram, K. Kuppusamy, and R. P. K. Devi, "Economic dispatch with prohibited operating zones using fast computation evolutionary programming algorithm," *Electr. Power Syst. Res.*, vol. 70, no. 3, pp. 245–252, Aug. 2004.
[28] L. dos Santos Coelho and V. C. Mariani, "Combining of chaotic differential evolution and quadratic programming for economic dispatch optimization with valve-point effect," *IEEE Trans. Power Syst.*, vol. 21, no. 2, pp. 989–996, May 2006.
[29] N. Amjady and H. Sharifzadeh, "Solution of non-convex economic dispatch problem considering valve loading effect by a new modified differential evolution algorithm," *Int. J. Elect. Power Energy Syst.*, vol. 32, no. 8, pp. 893–903, Oct. 2010.
[30] Y. Wang, J. Zhou, L. Mo, R. Zhang, and Y. Zhang, "Short-term hydrothermal generation scheduling using differential real-coded quantum-inspired evolutionary algorithm," *Energy*, vol. 44, no. 1, pp. 657–671, Aug. 2012.
[31] L. Mo, P. Lu, C. Wang, and J. Zhou, "Short-term hydro generation scheduling of three Gorges–Gezhouba cascaded hydropower plants using hybrid MACS-ADE approach," *Energy Convers. Manage.*, vol. 76, pp. 260–273, Dec. 2013.
[32] E. C. Finardi and M. R. Scuzziato, "Hydro unit commitment and loading problem for day-ahead operation planning problem," *Int. J. Elect. Power Energy Syst.*, vol. 44, no. 1, pp. 7–16, Jan. 2013.
[33] T. K. Siu, G. A. Nash, and Z. K. Shawwash, "A practical hydro, dynamic unit commitment and loading model," *IEEE Trans. Power Syst.*, vol. 16, no. 2, pp. 301–306, May 2001.
[34] L. Li and H. Tang, "Practical method of in-plant economical operation of Xi-Luo-Du hydropower plant with large number of generator sets," *Shuili Fadian Xuebao, J. Hydroelectr. Eng.*, vol. 35, no. 5, pp. 110–116, May 2016.
[35] J. Zhou, L. Yuan, P. Lu, Q. Qiao, L. Mo, and C. Wang, "Real-time load-adjusting method of cascade hydropower plants considering hydrological regime-changing conditions," *Shuili Fadian Xuebao, J. Hydroelectr. Eng.*, vol. 34, no. 9, pp. 1–9, Sep. 2015.
[36] P. Lu, J. Zhou, L. Mo, R. Zhang, and C. Wang, "An integrated dispatching mode for daily generation scheduling and inner-plant economic operation of cascade hydropower plants," *Dianwang Jishu, Power Syst. Technol.*, vol. 38, no. 7, pp. 1914–1922, 2014.
[37] S. Zhang, M. He, J. Gu, Z. Cui, J. Wang, L. Zhong, Q. Meng, and H. Wang, "Rock mass classification for columnar jointed basalt: A case study of baihetan hydropower station," *Geofluids*, vol. 2020, pp. 1–12, Dec. 2020.
[38] X. Ding, X. Niu, Q. Pei, S. Huang, Y. Zhang, and C. Zhang, "Stability of large underground caverns excavated in layered rock masses with steep dip angles: A case study," *Bull. Eng. Geol. Environ.*, vol. 78, no. 7, pp. 5101–5133, Oct. 2019.
[39] Y. Shang, S. Lu, Y. Ye, R. Liu, L. Shang, C. Liu, X. Meng, X. Li, and Q. Fan, "China' energy-water nexus: Hydropower generation potential of joint operation of the three Gorges and Qingjiang cascade reservoirs," *Energy*, vol. 142, pp. 14–32, Jan. 2018.
[40] C. Ma, J. Lian, and J. Wang, "Short-term optimal operation of Three-gorge and Gezhouba cascade hydropower stations in non-flood season with operation rules from data mining," *Energy Convers. Manage.*, vol. 65, pp. 616–627, Jan. 2013.
[41] X. Chen, J. Zhou, B. Jia, X. Yang, and C. Zhou, "Characterizing the hydraulic connection of cascade reservoirs for short-term generation dispatching via Gaussian process regression," *IEEE Access*, vol. 8, pp. 145489–145502, 2020.
[42] X. Guan, A. Svoboda, and C. Li, "Scheduling hydro power systems with restricted operating zones and discharge ramping constraints," *IEEE Trans. Power Syst.*, vol. 14, no. 1, pp. 126–131, Feb. 1999.
[43] C. Cheng, J. Wang, and X. Wu, "Hydro unit commitment with a head-sensitive reservoir and multiple vibration zones using MILP," *IEEE Trans. Power Syst.*, vol. 31, no. 6, pp. 4842–4852, Nov. 2016.
[44] C. Su, W. Yuan, C. Cheng, P. Wang, L. Sun, and T. Zhang, "Short-term generation scheduling of cascade hydropower plants with strong hydraulic coupling and head-dependent prohibited operating zones," *J. Hydrol.*, vol. 591, Dec. 2020, Art. no. 125556.
[45] B. Jia, J. Zhou, X. Chen, Z. He, Y. Zhang, and M. Tian, "Neural network estimation methods for varying output coefficients of hydropower stations," *Shuili Fadian Xuebao, J. Hydroelectr. Eng.*, vol. 40, no. 1, pp. 88–96, 2021.
[46] X. Chen, J. Zhou, B. Jia, Y. Yang, and L. Li, "An improved prediction method of water consumption rate considering aftereffects for short-term dispatching of hydropower station," in *Proc. E S Web Conf.*, vol. 199, 2020, Art. no. 00008.
[47] L. Yuan, J. Zhou, Z. Mai, and Y. Li, "Random fuzzy optimization model for short-term hydropower scheduling considering uncertainty of power load," *Water Resour. Manage.*, vol. 31, no. 9, pp. 2713–2728, Jul. 2017.

XIAO CHEN was born in Enshi, China, in 1993. He received the B.S. degree from the Huazhong University of Science and Technology (HUST), Wuhan, China, in 2017, where he is currently pursuing the Ph.D. degree in hydraulic and hydropower engineering.

His research areas include water resources modeling and optimization theory and method.

JIANZHONG ZHOU was born in Wuhan, China, in December 1959. He received the B.S. degree in automatic control from the Nanjing University of Aeronautics and Astronautics, Nanjing, China, in 1982.

He is currently a Professor with the School of Civil and Hydraulic Engineering, HUST. His research interests include optimal operation and control of hydropower energy systems.

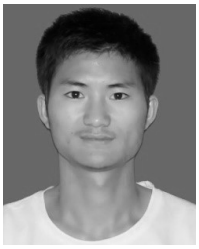

BENJUN JIA was born in Zunyi, China, in July 1994. He received the B.S. degree from the Huazhong University of Science and Technology (HUST), Wuhan, China, in 2017, where he is currently pursuing the Ph.D. degree in hydraulic and hydropower engineering.

His research interest includes modeling and operation theory in water resources management.